BJR

https://doi.org/10.1259/bjr.20190073

Received: 19 January 2019 | Revised: 20 April 2019 | Accepted: 29 April 2019

Cite this article as:
Zhang H, He X, Yu J, Song W, Liu X, Liu Y, et al. Preoperative MRI features and clinical laboratory indicators for predicting the early therapeutic response of hepatocellular carcinoma to transcatheter arterial chemoembolization combined with High-intensity focused ultrasound treatment. *Br J Radiol* 2019; **92**: 20190073.

FULL PAPER

Preoperative MRI features and clinical laboratory indicators for predicting the early therapeutic response of hepatocellular carcinoma to transcatheter arterial chemoembolization combined with High-intensity focused ultrasound treatment

[1]HAIPING ZHANG, BS, [1]XIAOJING HE, MD, [2]JIAYI YU, BS, [1]WENLONG SONG, BS, [1]XINJIE LIU, MD, [1]YANGYANG LIU, MD, [1]JUN ZHOU, MS and [1]DAJING GUO, MD

[1]Department of Radiology, the Second Affiliated Hospital of Chongqing Medical University, Chongqing, China
[2]Department of Radiology, Chongqing General Hospital, Chongqing, China

Address correspondence to: Mr Dajing Guo
E-mail: *guodaj@163.com*

The authors Haiping Zhang and Xiaojing He contributed equally to the work.

Objectives: To evaluate the value of preoperative MRI features and laboratory indicators in predicting the early response of hepatocellular carcinoma (HCC) to transcatheter arterial chemoembolization (TACE) combined with high-intensity focused ultrasound (HIFU) treatment and to establish a preoperative prediction model.

Methods: A total of 188 patients with 223 tumors who underwent TACE/HIFU treatment from January 2011 to June 2017 were included. Tumors were divided into three groups (< 2 cm, 2 – 5 cm,> 5 cm) and classified as non-complete response (NCR) and complete response (CR) cohorts according to the Response Evaluation Criteria in Cancer of the Liver (RECICL) 2015 revised version. Univariate analysis and multivariate logistic regression analysis were used to determine independent predictors, and receiver operating characteristic (ROC) curve analysis was performed to assess the diagnostic power of each predictor. The prediction model was derived on the β coefficient of the multivariate regression analysis of the predictors.

Results: Irregular margins in the 2 – 5 cm group were closely related to early NCR. Irregular margins, arterial peritumoral enhancement and abnormal alpha-fetoprotein (AFP) were independent predictors of early NCR in the > 5 cm group. The prediction model of this group suggests that irregular margins combined with arterial peritumoral enhancement and abnormal AFP combined with irregular margins and arterial peritumoral enhancement predict an increased risk of early NCR.

Conclusion: Irregular margins of 2 – 5 cm tumors and irregular margins, arterial peritumoral enhancement, and abnormal AFP of tumors > 5 cm can be applied to predict the early response of HCC to TACE/HIFU treatment.

Advances in knowledge: TACE combined with HIFU treatment may be able to significantly improve survival in patients with advanced HCC. Conventional MRI features and laboratory indicators are readily available without complex post-processing. It is feasible to predict the response of HCC after TACE/HIFU treatment based on preoperative conventional MRI features and laboratory indicators, the combination of multiple features predicts high-risk of non-complete response.

INTRODUCTION

Transcatheter arterial chemoembolization (TACE) has been widely used in hepatocellular carcinoma (HCC) patients at an intermediate-advanced stage; however, the complete necrosis rates were found to be only 17%~38%.[1,2] High-intensity focused ultrasound (HIFU) due to its minimal invasiveness and safety characteristics is becoming more widely used in the treatment of HCC to induce target lesion coagulation necrosis without damaging the surrounding structures.[3] It has been confirmed that TACE combined with HIFU (TACE/HIFU) may be able to

significantly improve the survival rate of HCC patients.[4] Nevertheless, residual tumors cannot be avoided after TACE/HIFU, and such tumors represent a hidden danger of recurrence. Therefore, it is essential to predict residual tumors preoperatively in HCC after TACE/HIFU treatment, which could help guide therapeutic strategies and greatly improve the prognosis of patients.

Imaging-based predictions that are noninvasive and repeatable can be used to assess the overall tumor response. Some studies have demonstrated that CT and MRI exhibit satisfactory results in predicting early responses in HCC,[5–7] especially MR functional imaging.[8,9] However, MR functional imaging is characterized by longer imaging time and is, thus, more affected by respiratory motion, the MR device, scan parameters, etc., which widely limits clinical applications. In contrast, given the stability and reproducibility, high-resolution images, and short imaging time of conventional MR, conventional MR features have potential applications in predicting tumor responses after TACE. According to study of Li Z et al[10] and Lee S et al,[6] tumor size was the most important predictive feature, although tumor enhancement was also effective predictor. Whether more detailed features, such as non-smooth tumor margins, arterial peritumoral enhancement, and rim enhancement, can be used for predicting tumor responses is worth further discussion. To our knowledge, with regard to HIFU or TACE/HIFU treatment, no study has reported the efficacy of predicting early HCC responses with conventional MR.

In addition to MR features, various clinical laboratory indicators have been confirmed to be effective in preoperative predictions. Previous studies demonstrated that serum alpha-fetoprotein (AFP) level not only has diagnostic value but also has predictive value for malignancy and prognosis of HCC.[11] Serum aspartate aminotransferase (AST), alanine aminotransferase and AFP levels were all significantly associated with disease-free survival (DFS) time in a univariate analysis of HCC after TACE.[12] However, the value of laboratory indicators in predicting the response of HCC after TACE/HIFU treatment remains unknown.

Due to lack of studies on predicting the response of HCC after TACE/HIFU treatment, the purpose of this retrospective study was to investigate the value of preoperative MRI features and laboratory indicators for predicting early responses of HCC after TACE/HIFU treatment and to establish a preoperative prediction model to guide therapeutic strategies and improve patient prognosis.

METHODS AND MATERIALS

Patients

This retrospective study was approved by the institutional review board, and the requirement to obtain written informed consent was waived.

The institutional database was collected from January 2011 to June 2017 to identify all patients with HCC who underwent TACE/HIFU. The inclusion criteria for our study were as follows: (1) patients with newly diagnosed HCC per the European Association for the Study of the Liver and the European Organization for Research and Treatment of Cancer (EASL-EORTC) criteria[13] with TACE/HIFU treatment; (2) with the exception of TACE/HIFU, no other surgery was performed; (3) patients with baseline contrast-enhanced MRI within 1 week before treatment. The exclusion criteria were as follows: (1) patients with diffuse HCC; (2) patients with follow-ups at less than 6 months or irregular follow-ups after treatment; (3) an MR image with significant artifacts that was not of sufficient quality for analysis.

A total of 532 patients were identified, and 256 patients without preoperative MRI or with images containing significant artifacts, 14 patients with diffuse HCC, and 74 patients with follow-ups at less than 6 months or irregular follow-ups after TACE/HIFU treatment were excluded. The final study population comprised 188 patients with 223 lesions; all tumors were divided into groups corresponding to tumor diameter smaller than 2 cm (group A), tumor diameter 2–5 cm (group B), and tumor diameter larger than 5 cm (group C).

MRI data acquisition

At 1 week before and 1 week, 2–3 months, and 5–6 months after TACE/HIFU treatment, MR images were acquired using a 1.5T MR scanner (HDXT2012, GE Medical Systems, Fairfield, CT). Axial in-phase and out-phase T_1 weighted image, axial fat-suppressed T_2 weighted image, axial and coronal breath-hold contrast-enhanced fat-suppressed T_1 weighted image were provided for our imaging protocols, Gadodiamide (Omniscan, GE Healthcare, Co.Cork, Ireland) was injected in contrast-enhanced scans for a total dose of 0.2 mL/kg body weight. Enhanced arterial phase, portal venous phase and delayed phase data were obtained at 25–30, 60–65 and 180–200 sec after contrast injection. All MRI parameters are listed in Table 1; the sequences and parameters were consistent before and after treatment.

Table 1. MR Imaging Parameters

Sequence	TR (msec)	TE (msec)	Bandwidth (KHz)	Slice thickness (mm)	Interslice gap (mm)	FOV (cm ×cm)	Matrix size
Axial in-phase T_1 FSPGR	220	4.7	62.5	7	1	42 × 33.6	288 × 160
Axial out-phase T_1 FSPGR	220	2.1	62.5	7	1	42 × 33.6	288 × 160
Axial FS T_2 FSE	6316	90.9	41.7	7	1	44 × 35.2	288 × 224
Contrast-enhanced FS T_1 3D-LAVA	4.2	2.0	83.3	4.8 ~ 5.4	−1.4 ~ −2.7	42 × 33.6	320 × 192

Notes: FSPGR = fast spoiled gradient-echo; FS = fat-suppressed; FSE = fast spin-echo; 3D-LAVA = three-dimensional liver acquisition with volume acceleration; TR = repetition time; TE = echo time; FOV = field of view.

Table 2. Baseline Clinical Characteristics of the Study Population

Laboratory indicators	<2 cm			2–5 cm			>5 cm		
	CR (n = 21)[a]	NCR (n = 6)[a]	P	CR (n = 48)[a]	NCR (n = 31)[a]	P	CR (n = 37)[a]	NCR (n = 45)[a]	P
Mean age (y)[b]	50.5 ± 10.4	50.0 ± 17.2	0.951	52.8 ± 11.8	50.6 ± 11.5	0.420	52.1 ± 10.2	52.8 ± 10.4	0.752
M/F ratio	18/3	6/0	1.000	40/8	26/5	0.950	32/5	39/6	1.000
HBV (± ratio)	19/2	6/0	1.000	46/2	31/0	0.517	34/3	42/3	1.000
AFP			0.101			0.401			0.020
≤13.2 μg l^{-1}	3 (14.3)	3 (50.0)		15 (31.3)	7 (22.6)		13 (35.1)	6 (13.3)	
>13.2 μg l^{-1}	18 (85.7)	3 (50.0)		33 (68.7)	24 (77.4)		24 (64.9)	39 (86.7)	
ALT[b]	68.0 (29.5,128.0)	43.0 (39.5,450.3)	0.620	42.0 (25.0,95.5)	51.0 (33.5,104.0)	0.322	51.0 (34.0,133.0)	58.0 (35.0,111.0)	0.908
AST[b]	44.0 (34.5,105.5)	70.5 (31.0,203.8)	0.484	39.0 (28.3,85.8)	42.0 (30.0,75.5)	0.718	55.0 (33.0,99.0)	51.0 (37.0,94.0)	0.843
γ-GT[b]	73.0 (40.5,172.5)	63.0 (43.8,117.5)	0.641	53.5 (32.0,102.5)	69.0 (42.5,124.5)	0.507	138.0 (62.5,194.0)	141.0 (102.0,257.0)	0.141
ALP[b]	102.0 (75.5,121.5)	129.0 (103.0,231.8)	0.129	109.1 ± 55.1	109.5 ± 48.9	0.978	132.0 (99.5,174.0)	135.0 (103.0,187.0)	0.463
PT[b]	14.7 ± 1.9	15.8 ± 2.6	0.268	14.0 (13.4,14.9)	13.8 (13.1,14.6)	0.320	13.9 (13.2,14.5)	13.8 (13.0,14.7)	0.839
Alb[b]	39.2 ± 4.5	38.8 ± 6.9	0.886	40.2 (36.6,42.9)	39.1 (37.1,43.7)	0.840	38.0 (32.9,42.0)	37.7 (34.2,41.5)	0.931
SCr[b]	72.7 ± 17.3	75.8 ± 15.0	0.697	75.9 (66.8,81.8)	72.8 (66.1,86.5)	0.851	69.5 ± 17.4	71.2 ± 17.0	0.660
RBC[b]	4.2 ± 0.5	4.0 ± 0.6	0.423	4.6 (4.0,4.6)	4.5 (3.9,4.8)	0.744	4.5 ± 0.6	4.4 ± 0.7	0.537
WBC[b]	4.5 ± 1.8	4.1 ± 2.2	0.629	5.4 (3.6,6.3)	5.0 (4.2,5.7)	0.411	6.5 ± 2.8	6.2 ± 2.6	0.653
PLT[b]	80.0 (58.0,101.0)	86.5 (32.5,115.3)	0.930	93.5 (61.3,133.0)	116.0 (78.5,154.0)	0.120	140.0 (114.5,192.0)	121.0 (96.0,182.0)	0.313
T-Bil[b]	13.8 (10.0,20.9)	23.9 (12.7,125.9)	0.221	15.4 (11.9,22.3)	15.3 (11.9,23.6)	0.904	13.7 (11.2,20.8)	15.2 (11.4,17.7)	0.746
Hepatic fibrosis									
PC III[b]	11.1 ± 5.5	18.8 ± 10.0	0.019	10.4 (7.4,13.3)	9.4 (6.7,13.7)	0.865	11.1 (8.0,16.9)	11.7 (9.4,15.4)	0.714
IV-C[b]	69.9 (44.4,130.4)	207.2 (38.4,664.8)	0.382	79.5 (51.9,140.9)	61.9 (41.4,122.3)	0.306	92.5 (62.3,139.6)	106.6 (68.4,140.7)	0.588
LN[b]	119.3 ± 60.1	144.2 ± 89.2	0.164	80.6 (48.3,149.5)	83.8 (59.2,115.1)	0.996	127.7 ± 62.8	130.5 ± 65.3	0.857
HA[b]	89.9 (54.8,222.0)	417.4 (99.9,913,8)	0.080	107.6 (52.5,212.4)	111.7 (59.5,168.9)	0.971	117.9 (74.4,189.4)	89.4 (54.3,150.6)	0.330
Child-Pugh			0.588			0.438			1.000
A	17 (81.0)	4 (66.7)		43 (89.6)	26 (84.8)		33 (89.2)	40 (88.9)	
B	4 (19.0)	2 (33.3)		4 (8.3)	2 (6.1)		4 (10.8)	5 (11.1)	
C	0 (0)	0 (0)		1 (2.1)	3 (9.1)		0	0	

CR, complete response; NCR, non-complete response; M/F, Male/Female; HBV, hepatitis B virus; AFP, alpha-fetoprotein; ALT, alanine aminotransferase; AST, aspartate aminotransferase; γ-GT=γ-glutamyl transferase; ALP, alkaline phosphatase; PT, prothrombin time; Alb, albumin; SCr, serum creatinine; RBC, red blood cell count; WBC, white blood cell count; PLT, platelet count; PC III, procollagen III; IV-C, collagen IV; LN, laminin; HA, hyaluronic acid.

Notes Unless otherwise indicated, data are the number of patients with the percentage in parentheses.

[a]Non-assessable (NA) values were excluded; 9 tumors of CR and 5 tumors of NCR in group A, 13 tumors of CR and 7 tumors of NCR in group B, and 1 tumors of CR in group C were marked as NA.

[b]Continuous variables: normally distributed data are reported as the means ± standard deviations, and non-normally distributed data are reported as medians with interquartile ranges in parentheses (25th, 75th percentiles).

Table 3. Radiologic Characteristics of the Study Lesions

Preoperative MRI feature	<2 cm			2–5 cm			>5 cm		
	CR(n = 30)	NCR(n = 11)	P	CR(n = 61)	NCR(n = 38)	P	CR(n = 38)	NCR(n = 45)	P
Tumor size[a]	1.4 ± 0.3	1.4 ± 0.4	0.925	3.0 ± 0.8	3.3 ± 0.8	0.079	8.1 ± 2.5	9.1 ± 3.0	0.140
Minimum distance	1.4 (0.0,3.1)	0.8 (0.0,1.3)	0.120	0.0 (0.0,2.1)	0.9 (0.0,3.0)	0.199	0.0 (0.0,0.6)	0.0 (0.0,0.0)	0.084
Location			0.706			0.817			0.704
Right	20 (66.7)	7 (63.6)		46 (6.6)	27 (71.1)		24 (63.2)	25 (55.6)	
Left	9 (30.0)	3 (27.3)		11 (18.0)	9 (23.7)		6 (15.8)	7 (15.6)	
Junction	1 (3.3)	1 (9.1)		4 (75.4)	2 (5.3)		8 (21.1)	13 (28.9)	
Number			0.607			0.211			0.596
1	18 (60.0)	5 (45.5)		36 (59.0)	26 (68.4)		35 (92.1)	41 (91.1)	
2	8 (26.7)	5 (45.5)		12 (19.7)	9 (23.7)		1 (2.6)	3 (6.7)	
3	4 (13.3)	1 (9.1)		13 (21.3)	3 (7.9)		2 (5.3)	1 (2.2)	
Irregular margin			1.000			<0.001			<0.001
Smooth	19 (63.3)	7 (63.6)		43 (70.5)	10 (26.3)		18 (47.4)	1 (2.2)	
Irregular	11 (36.7)	4 (36.4)		18 (29.5)	28 (73.7)		20 (52.6)	44 (97.8)	
Arterial peritumoral enhancement			1.000			0.041			<0.001
Absent	27 (90.0)	10 (90.9)		51 (83.6)	25 (65.8)		26 (68.4)	8 (17.8)	
Present	3 (10.0)	1 (9.1)		10 (16.4)	13 (34.2)		12 (31.6)	37 (82.2)	
Rim enhancement			0.170			0.013			0.890
Absent	29 (96.7)	9 (81.8)		44 (72.1)	18 (47.4)		20 (52.6)	23 (51.1)	
Present	1 (3.3)	2 (18.2)		17 (27.9)	20 (52.6)		18 (47.4)	22 (48.9)	
Satellite nodules			1.000			0.031			0.089
Absent	29 (96.7)	11(100)		56 (91.8)	29 (76.3)		24 (63.2)	20 (44.4)	
Present	1 (3.3)	0 (0)		5 (8.2)	9 (23.7)		14 (36.8)	25 (55.6)	
PV/HV invasion			1.000			0.105			0.005
Absent	24 (80.0)	9 (81.8)		49 (80.3)	25 (65.8)		14 (36.8)	5 (11.1)	
Present	6 (20.0)	2 (18.2)		12 (19.7)	13 (34.2)		24 (63.2)	40 (88.9)	
Intratumoral artery			1.000			0.034			0.009
Absent	26 (86.7)	10 (90.9)		39 (63.9)	16 (42.1)		12 (31.6)	4 (8.9)	
Present	4 (13.3)	1 (9.1)		22 (36.1)	22 (57.9)		26 (68.4)	41 (91.1)	
Radiological capsule			0.153			0.508			0.074
Absent	14 (46.6)	9 (81.8)		22 (36.1)	15 (39.5)		14 (36.8)	25 (55.6)	
Partial	5 (16.7)	9 (9.1)		18 (29.5)	14 (36.8)		17 (44.7)	18 (40.0)	
Complete	11 (36.7)	1 (9.1)		21 (34.4)	9 (23.7)		7 (18.4)	2 (4.4)	
Lipoid			0.496			0.535			0.531
Absent	26 (86.7)	11(100)		38 (62.3)	26 (68.4)		32 (84.2)	40 (88.9)	
Present	4 (13.3)	0 (0)		23 (37.7)	12 (31.6)		6 (15.8)	5 (11.1)	
Hemorrhage			1.000			0.359			0.800
Absent	30(100)	11(100)		53 (86.9)	36 (94.7)		23 (60.5)	26 (57.8)	
Present	0 (0)	0 (0)		8 (13.1)	2 (5.3)		15 (39.5)	19 (42.2)	
Ascites			0.942			0.362			0.157
Absent	24 (80.0)	8 (72.7)		51 (83.6)	35 (92.1)		32 (84.2)	32 (71.1)	

(Continued)

Table 3 (Continued)

Preoperative MRI feature	<2 cm		P	2–5 cm		P	>5 cm		P
	CR(n = 30)	NCR(n = 11)		CR(n = 61)	NCR(n = 38)		CR(n = 38)	NCR(n = 45)	
Present	6 (20.0)	3 (27.3)		10 (16.4)	3 (7.9)		6 (15.8)	13 (28.9)	
Portal hypertension			0.796			0.432			0.310
Absent	15 (50.0)	5 (45.5)		24 (39.3)	18 (47.4)		23 (60.5)	32 (71.1)	
Present	15 (50.0)	6 (54.5)		37 (60.7)	20 (52.6)		15 (39.5)	13 (28.9)	

CR, complete response; NCR, non-complete response; PV/HV, portal vein/hepatic vein. Minimum distance is defined as the minimum distance between the liver envelope and the edge of the tumor.
Notes Unless otherwise indicated, data are the number of tumors with the percentage in parentheses.
[a]Continuous variables: normally distributed data are reported as the means ± standard deviations, and non-normally distributed data are reported as medians with interquartile ranges in parentheses (25th, 75th percentiles).

Figure 1. A 58-year-old female with HCC in the NCR group. A and B, The tumor with a maximum diameter of 1.6 cm had an irregular margin (white arrow) in the arterial phase and the portal venous phase on preoperative MR imaging. C and D, One week after TACE/HIFU treatment, the tumor had no enhancement in the arterial phase or the portal venous phase. E and F, Six months after TACE/HIFU treatment, lesions with enhanced nodule (white arrow) in the arterial phase and washout (white arrow) in the portal venous phase demonstrated the recurrence of HCC.

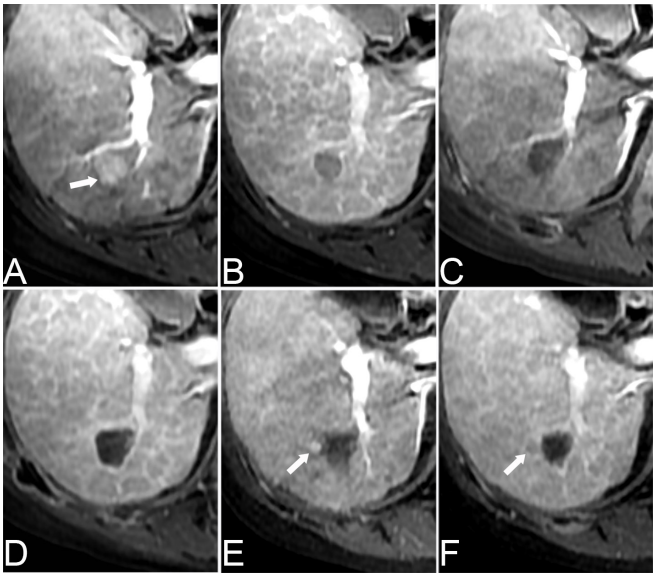

Image analysis

MR images were retrospectively evaluated by two radiologists with more than 8 years of experience in hepatic MR imaging who were unaware of information regarding the clinical, laboratory, imaging report, and follow-up results. The two observers independently evaluated the following MRI features for each HCC: (1) tumor size; (2) minimum distance between tumor and liver capsule; (3) location; (4) number; (5) irregular margin; (6) arterial peritumoral enhancement; (7) rim enhancement; (8) satellite nodules; (9) portal vein (PV) or hepatic vein (HV) invasion; (10) intratumoral artery; (11) radiological capsule; (12) intratumoral lipoid; (13) intratumoral hemorrhage; (14) ascites; and (15) portal hypertension.

After the first independent image evaluation, interobserver agreement was assessed. Any discrepancies in the results between the two radiologists were resolved by consensus of the two observers.

Clinical laboratory indicators

All threshold values chosen for laboratory indicators were based on the normal ranges used at our institution. Clinical factors potentially related to early therapeutic response included age; gender; hepatitis B surface antigen (HBsAg) status (positive or negative); AFP level (ug/L); alanine aminotransferase (ALT; U/L); aspartate aminotransferase (AST; U/L); γ-glutamyl transferase (γ-GT; U/L); alkaline phosphatase (ALP; U/L); prothrombin time (PT; s); albumin (Alb; g/L); serum creatinine (SCr; Umol/L); red blood cell count (RBC; 10^{12}/L); white blood cell count (WBC; 10^{9}/L); platelet count (PLT; 10^{9}/L); hepatic fibrosis spectrum and Child-Pugh grade (A, B or C). If the patients had more than one tumor, the laboratory data of the smaller tumor were marked as not assessable (NA).

TACE treatment

TACE treatment was achieved in an operating room with a digital subtraction angiography (DSA) device (INFX-8000, Toshiba Medical Systems, Otawara, Japan) by two experienced interventional radiologists (both with more than 5 years of clinical practice). After identifying the supportive artery by angiography of the abdominal aorta, an emulsion consisting of lipiodol (10–25 ml), pirarubicin (20–40 mg) and lobaplatin (50 mg) was injected into the feeding artery through a 2.7 F microcatheter. For some HCCs with an excessive blood supply, a gelatin sponge or polyvinyl alcohol particle was used to support further embolization until the tumor-feeding artery was essentially blocked and the staining completely vanished.

HIFU ablation

HIFU treatment for each patient was performed 2 to 3 weeks after TACE treatment. Before the treatment began, the skin of patient was cleaned by degassed water, and a vacuum suction

Figure 2. A 40-year-old female with HCC in the NCR group. A, The tumor with a maximum diameter of 4.3 cm had peritumoral enhancement (white arrow) in the arterial phase on preoperative MR imaging. B, Peritumoral enhancement was isointense with the background liver parenchyma in the portal venous phase. C and D, One week after TACE/HIFU treatment, the tumor had no enhancement in the arterial phase or the portal venous phase. E and F, Six months after TACE/HIFU treatment, enhanced tissue on MR imaging indicated the recurrence of HCC.

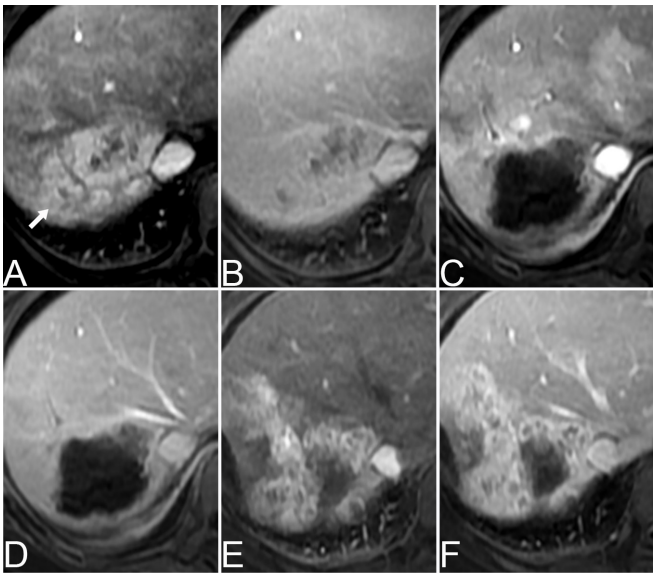

device was used to degas the skin. All patients were anesthetized to minimize the effects of the movement caused by breathing on liver displacement. Treatment was administered with a JC-type focused ultrasound tumor therapy system (Chongqing HIFU Technology Co., Ltd., Chongqing, China) consisting of an ultrasonic real-time monitoring and a three-dimensional scanning treatment system. Therapeutic ultrasound energy was produced by a transducer operating at 0.8 MHz (aperture 120 mm, focal length 135 mm). The location, size, and boundary of the tumors were determined by an integral central 3.5–5.0-MHz diagnostic ultrasound probe (Esaote, Genoa, Italy), and the treatment pathway and target areas were then confirmed. The tumour was divided into 5 mm sections, and the tumor tissue in each section was completely ablated by moving the therapeutic probe under the real-time monitoring of ultrasonographic imaging; this process was repeated until the target area was completely ablated. The lesion sizes were measured before, during and after treatment to determine the treatment range. The gray-scale changes in the ablation site were observed to determine if the lesion had reached the target of necrosis, and skin temperature was monitored regularly to prevent thermal injury during the course of ablation.

Postoperative efficacy evaluation

Postoperative efficacy was evaluated by two additional radiologists. Any discrepancies were resolved by further joint assessment until a consensus was reached. The postoperative efficacy of all HCC lesions was evaluated by referencing the Response Evaluation Criteria in Cancer of the Liver (RECICL) 2015 revised version,[14] the evaluation criteria were as follows: (1) treatment effect 4(TE4), defined as 100% tumor-necrotizing effect or 100% tumor size reduction; (2) TE3, defined as 50–100% tumor necrosis or 50–100% reduction in tumor size; (3) TE2, defined as effect neither TE3 nor TE2; and (4) TE1, defined as more than 50% tumor enlargement excluding the area of necrosis after treatment. Generally, lesions with hypervascular tissue in the arterial phase and washout in the portal venous or delayed phases within 6 months of review after treatment were considered to require further clinical intervention. Therefore, TE1, TE2 and TE3 were classified as non-complete responses (NCRs), and TE4 was classified as a CR.

Statistical analysis

Interobserver agreement about the existence of MRI features was evaluated by the Cohen κ coefficient. The Kolmogorov-Smirnov test was first used to test the normal distribution of continuous variables. Two-sample t-tests were used for normally distributed data, and the Mann-Whitney U test was used to check for non-normally distributed data. Categorical variables were analyzed using the chi-squared test or the Fisher exact test. Statistical differences among multiple groups were analyzed using ANOVA.

A multivariate analysis was used to determine independent predictors among the MRI characteristics and laboratory indicators. Variables with a P value < 0.1 were entered into the multivariate logistic regression analysis to establish the preoperative prediction model. Receiver operating characteristic (ROC) curves were generated, and the area under the curve (AUC) was calculated to evaluate the diagnostic power of each predictor. The sensitivity, specificity, positive predictive value (PPV), and negative predictive value (NPV) of predictors were also calculated.

A clinical prediction model was established on the basis of multivariate logistic regression analysis. The score of each valuable independent predictor was determined according to the β coefficient.[15] The variable with the maximum β value was assigned a score of 10, and the other variables were assigned corresponding scores based on the ratio of the maximum β value. The cutoff value and AUC of the predictive scoring model were determined by the ROC curve. The sensitivity, specificity, PPV, and NPV were calculated.

All statistical analyses were performed using SPSS software version 22 (IBM Corporation, Armonk, NY). A two-tailed P value < 0.05 was considered indicative of a statistically significant difference.

RESULTS

Baseline clinical and radiologic characteristics of the patients

There were 223 tumors in 188 patients. Among these, 161 patients had single lesions, 19 had two lesions, and eight had three lesions. 45 lesions were located in the left lobe of the liver, 149 lesions were located in the right lobe, and 29 lesions were

Figure 3. A 52-year-old male with HCC in the NCR group. A and B, The tumor with a maximum diameter of 3.0 cm had irregular margins (white arrow) on preoperative MR imaging. C and D, One week after TACE/HIFU treatment, the tumor had no enhancement in the arterial phase or the portal venous phase. E and F, Five months after TACE/HIFU treatment, enhanced tissue around the tumor (white arrow) demonstrated the recurrence of HCC.

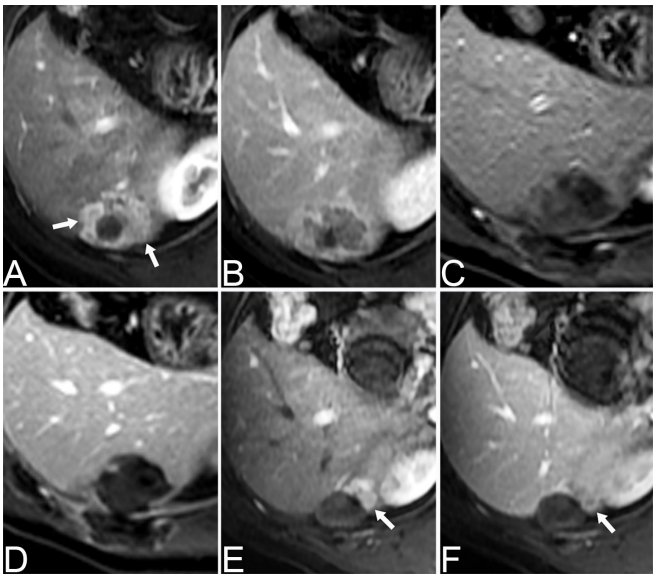

located in the junction. The mean maximum tumor diameter was 4.8 ± 3.5 cm. The baseline clinical characteristics of the study population are summarized in Table 2. The radiologic characteristics of the study lesions are summarized in Table 3.

Treatment response

After TACE/HIFU treatment, 11 NCR lesions (11/41, 26.8%) (Figure 1) in group A, 38 NCR lesions (38/99, 38.4%) (Figures 2 and 3) in group B, and 45 NCR lesions (45/83, 54.2%) in group C were evaluated with reference to RECICL 2015 revised version. The rate of NCR was significantly different among the three groups ($p < 0.05$); as the diameter of the tumor increased, the rate of NCR increased.

Predictors for NCR based on univariate analysis and multivariate logistic regression analysis

As shown in Table 4, in group A, only the laboratory indicators of type III procollagen (PC III) ($p = 0.019$) and hyaluronic acid (HA) ($p = 0.080$) were predictive of an early response according to the univariate analysis; there were no significant differences in MRI features ($p > 0.1$). The multivariate logistic regression analysis showed that neither PC III ($p = 0.248$) nor HA ($p = 0.442$) were independent predictors. In group B, there were no significant differences in laboratory indicators according to the univariate analysis ($p > 0.1$). MRI features, including tumor size, irregular margins, arterial peritumoral enhancement, rim enhancement, satellite nodules and intratumoral artery, met the criteria for inclusion in the multivariate logistic regression analysis ($p = 0.079$, $p < 0.001$, $p = 0.041$, $p = 0.013$, $p = 0.031$ and $p = 0.034$), and only an irregular margin ($p = 0.001$) was a significant independent predictor of early NCR. In group C, the univariate analysis indicated that an irregular margin, arterial peritumoral enhancement, satellite nodules, PV/HV invasion, intratumoral artery, radiological capsule, minimum distance, and abnormal AFP values satisfied the conditions for inclusion in the multivariate logistic regression analysis ($p < 0.001$, $p < 0.001$, $p = 0.089$, $p = 0.005$, $p = 0.009$, $p = 0.074$, $p = 0.084$ and $p = 0.020$), and the results showed that an irregular margin ($p = 0.020$), arterial peritumoral enhancement ($p = 0.022$), and abnormal AFP values ($p = 0.042$) were significant independent predictors of early NCR. Interobserver agreement for the presence of an irregular margin and arterial peritumoral enhancement was good ($\kappa = 0.75$ and 0.68).

Predictive performance of the predictors

The ROCs of irregular margins in group B and irregular margins, arterial peritumoral enhancement, AFP values in group C are shown in Figure 4A and B, and the area under the ROC curve (AUROC), sensitivity, specificity, PPV and NPV are shown in Table 5.

Prediction model for NCR

According to the multivariate logistic regression analysis, there was no independent predictor in group A, only one independent predictor in group B, and three independent predictors in group C. Therefore, a prediction model was established only in group C based on the three significant predictors. The scoring methods for each valuable predictor are shown in Figure 5, which indicated that arterial peritumoral enhancement combined with irregular margins, abnormal AFP values combined with arterial peritumoral enhancement, and irregular margins were high-risk factors for NCR (cutoff = 16.5). The prediction model had good diagnostic performance (AUROC = 0.844, 95% CI: 0.756–0.933, as shown in Figure 4C), and the sensitivity, specificity, PPV and NPV of the prediction model were 82.2% (37/45), 73.7% (28/38), 78.7% (37/47) and 77.8% (28/36), respectively.

DISCUSSION

In our study, we assessed the value of preoperative MRI features and laboratory indicators for predicting the early response of HCC to TACE/HIFU treatment. There were no significant predictors of NCR in HCC with a diameter of less than 2 cm, only an irregular margin was an independent predictor of NCR in HCC with a diameter between 2 and 5 cm, and arterial peritumoral enhancement, irregular margins, and abnormal AFP values were independent predictors of NCR in HCC larger than 5 cm in diameter. These independent predictors displayed good predictive performance for NCR. We also established a prediction model for HCC with a diameter >5 cm, arterial peritumoral enhancement combined with irregular margins, abnormal AFP values combined with arterial peritumoral enhancement and irregular margins were significant predictors of tumors with a high-risk of NCR.

Previous studies have demonstrated that tumor size is associated with postoperative prognosis of HCC.[10,16] Size was also an important factor in local treatment such as TACE, RF and

Table 4. Univariate and Multivariate Analysis of Preoperative MR Features and Laboratory Indicators for Predicting Early NCR of HCC

	Univariate analysis	Multivariate analysis				
	P	β	SE	*P*	OR	95% CI
<2 cm						
Procollagen III	0.019	0.098	0.085	0.248	1.103	0.934–1.304
Hyaluronic acid	0.080	0.001	0.001	0.442	1.101	0.998–1.004
2–5 cm						
Tumor size	0.079	−0.063	0.341	0.852	0.939	0.481–1.831
Irregular margin	<0.001	1.672	0.495	0.001	5.324	2.018–14.045
Arterial peritumoral enhancement	0.041	0.324	0.594	0.585	1.383	0.432–4.426
Rim enhancement	0.013	0.733	0.519	0.158	2.081	0.752–5.757
Satellite nodules	0.031	0.681	0.692	0.326	1.975	0.508–7.671
Intratumoral artery	0.034	0.519	0.499	0.298	1.681	0.632–4.468
>5 cm						
Irregular margin	<0.001	2.621	1.123	0.020	13.753	1.522–124.267
Arterial peritumoral enhancement	<0.001	1.831	0.799	0.022	6.241	1.304–29.864
Satellite nodules	0.089	0.349	0.630	0.579	1.418	0.413–4.870
PV/HV invasion	0.005	0.370	0.807	0.646	1.448	0.298–7.043
Intratumoral artery	0.009	−0.149	0.941	0.875	0.862	0.136–5.453
Radiological capsule	0.074	0.100	0.547	0.854	1.106	0.378–3.233
Minimum distance	0.084	−0.277	0.222	0.211	0.758	0.491–1.170
alpha-fetoprotein	0.020	1.576	0.773	0.042	4.838	1.062–22.028

Notes Variables with a *P* value < 0.1 according to the univariate analysis were entered into the multivariate analysis.
Minimum distance is defined as the minimum distance between the liver envelope and the edge of the tumor.
β, partial regression coefficient; SE, Standard Error; OR, odds ratio; CI, confidence interval; PV/HV, portal vein/hepatic vein.

HIFU. Therefore, we classified the tumors into three groups according to the grouping standard of Renzulli M et al[17] to reduce the direct impact of tumor size on the assessment of predictors. We found that tumor size of CR and NCR were not statistically significant in each group, proving that our experimental design was effective. Thus, we successfully avoided the dominant effect of size in the tumor response by grouping. As shown in the treatment response results, the rate of NCR in group A, group B, and group C was 26.8%, 38.4%, and 54.2%, which indicated that the rate of NCR increased as the diameter of the tumor increased. The NCR rate of HCC in group A was higher than those of surgical resection[18] and radiofrequency ablation.[19] This discrepancy may be attributed to the heterogeneity of the HCCs evaluated. In our study, nearly half of the HCC patients in group A had more than one lesion (18/41, 43.9%), and most lesions had more than one potential malignant characteristic, such as irregular margins, arterial peritumoral enhancement, or absence of a capsule. In addition, our patients lived in an area with a high incidence of hepatitis B and cirrhosis, and group A had a small sample size. Nonetheless, in

Figure 4. The ROC curves of each independent predictor and prediction model. A, ROC curve of irregular margins in group B. B, ROC curves of arterial peritumoral enhancement, irregular margins, and alpha-fetoprotein in group C. C, ROC curve of the prediction model in group C. AUROC = area under receiver operating characteristic.

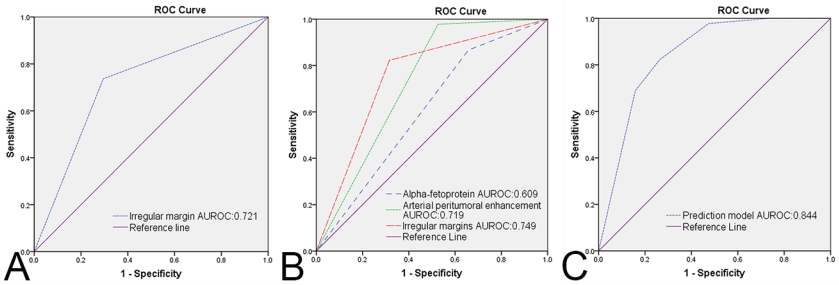

Figure 5. Prediction model of early NCR based on the β value of the predictors in group C. The scores for each predictor and combined predictors (upper section) and the diagnostic performance of the prediction model (lower section). AFP = alpha-fetoprotein; APE = arterial peritumoral enhancement; IM = irregular margin; β = partial regression coefficient; AUROC = area under receiver operating characteristic; CI = confidence interval; PPV = positive predictive value; NPV = negative predictive value.

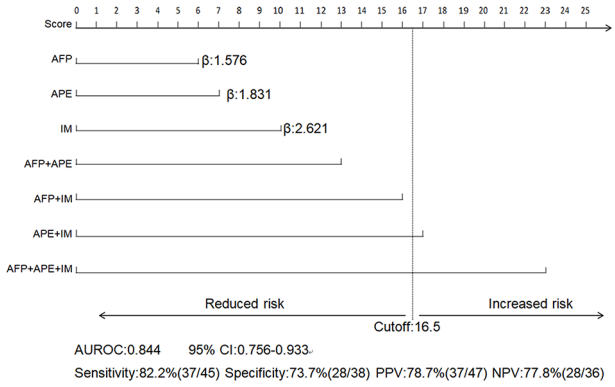

group C, which had the highest NCR rate, the NCR rate was still lower than that of TACE treatment alone.[1,2]

A previous study verified that irregular margins can predict microscopic portal vein invasion, intrahepatic metastasis, and early recurrence after hepatectomy in patients with HCC.[20] Our multivariate logistic regression analysis also showed significant predictive value for the treatment response in groups B and C (p = 0.001, p = 0.020). Irregular margins indicated more frequent MVI and poorer biological behavior, which were therefore a valuable predictor of treatment response in larger lesions. However, there was no significant difference in irregular margins (p = 1) in group A, which may be associated with a lower detection rate (36.6%, 15/41). The incidence of irregular margins increased as the tumor size increased (46.5%, 46/99 in group B; 77.1%, 64/83 in group C). Therefore, the appearance of irregular margins in tumors > 2 cm suggests that expanding the area of ablation should be considered to reduce the risk of NCR.

In a study of early relapse after surgical resection of liver cancer, An C et al[21] verified that arterial peritumoral enhancement was predictive of risk. Several other studies have also widely confirmed arterial peritumoral enhancement as an independent predictor of MVI,[17,22] which is well known as the most important risk factor for the early recurrence of liver cancer.[23] In our study, arterial peritumoral enhancement was also demonstrated to predict NCR after TACE/HIFU treatment in group C. There was a significant difference in arterial peritumoral enhancement in group B (p = 0.041) according to the univariate analysis, indicating that arterial peritumoral enhancement also had an increasing trend in NCR. There was no significant difference in group A (p = 1), which might be related to the small sample size (n = 41) and the low incidence of arterial peritumoral enhancement in the small lesions (9.8%, 4/41). Matsui O et al[24] and Choi JY et al[25] hypothesized that arterial peritumoral enhancement might be due to a microscopic tumor thrombus around the tumor blocking the minute portal vein branch, further leading to compensatory arterial hyperperfusion in the area of decreased or absent portal venous flow. Therefore, we speculate that because ultrasound enhancement cannot be exploited during the treatment of TACE/HIFU, the abnormal perfusion around the tumor cannot be detected by conventional real-time ultrasonography. Thus, the ablation range will not be expanded, which may lead to increased tumor recurrence in the short term. Therefore, it is necessary for clinicians to alert the occurrence of arterial peritumoral enhancement and to consider expanding ablation and short-term review for tumors > 5 cm.

Previous research on TACE clarified that a higher AFP value was an independent risk factor for tumor recurrence and metastasis.[26,27] In our study, abnormal AFP values were demonstrated to be a significant predictor only in group C, but not in the other two groups. AFP is secreted by cancerous or regenerated hepatocytes,[28] and decreasing AFP values after transarterial therapies were considered to be the result of tumor hypoxia and necrosis[29] and were thought to indicate a positive response to treatment.[30] Therefore, abnormal AFP values were not significant predictors in the smaller group due to high rate of CR. However, the NCR rate in group C was higher, and the residual tumor tissue might persistently secrete AFP after treatment.[31] In addition, because of the longer ablation time and the wider range of HIFU ablation treatment in the large tumor group, the inflammatory response of the surrounding hepatocytes, which may also secrete AFP continuously, was more severe.

Table 5. Diagnostic Performance of Preoperative MR Features and Laboratory Indicators for Predicting Early NCR of HCC

	AUROC	95% CI	Sensitivity	Specificity	PPV	NPV
2–5 cm						
IM	0.721	0.616–0.826	73.7 (28/38)	70.5 (43/61)	60.9 (28/46)	81.1 (43/53)
>5 cm						
IM	0.749	0.638–0.860	97.8 (44/45)	47.4 (18/38)	68.8 (44/64)	94.7 (18/19)
APE	0.719	0.602–0.835	82.2 (37/45)	68.4 (26/38)	75.5 (37/49)	76.5 (26/34)
AFP	0.609	0.484–0.734	86.7 (39/45)	35.1 (13/37)	61.9 (39/63)	68.4 (13/19)

AUROC, area under receiver operating characteristic; CI, confidence interval; PPV, positive predictive value; NPV, negative predictive value; IM, irregular margin; APE, arterial peritumoral enhancement; AFP, alpha-fetoprotein.

Some limitations of our research must be noted. First, this was a single-center, retrospective study with inevitable optional bias, as the results do not represent all types of liver cancer. Second, because of incomplete data, gadolinium ethoxybenzyl diethylenetriaminepentaacetic acid (Gd-EOB-DTPA) enhancement was not able to be applied, which affected the evaluation of the MRI features such as tumor size, irregular margins, satellite nodules, etc. Third, our prediction model was primarily aimed at tumors larger than 5 cm but lacked a validation group. The results were limited by the number of patients, and tumors larger than 5 cm failed to be further grouped. In addition, the suitability for HCC diameters less than 5 cm requires further validation. Finally, the CR rate after HIFU/TACE treatment in our study was not ideal. MRI-guided focused ultrasound (MRgFUS), a technology that combines thermal ablation with the anatomic, functional, and thermal guidance with MRI methods,[32] has superior soft tissue resolution for displaying the details of the tumor as well as an exquisite relationship with surrounding tissues such as blood vessels, and allows timely and exact control of the achievement of thermal necrosis, which is more accurate than ultrasound through grayscale changes in assessing the ablation degree. However, liver movements may significantly affect lesions targeting and ablation efficacy of MRgFUS. Further confirmation is needed to determine whether MRgFUS will overcome the limits of US-guided procedures in increasing the CR rate of lesions.

In conclusion, our study indicated that irregular margins of 2–5 cm tumors and irregular margins, arterial peritumoral enhancement, and abnormal AFP values of tumors > 5 cm are independent predictors of early NCR. Furthermore, arterial peritumoral enhancement combined with irregular margins; and abnormal AFP combined with arterial peritumoral enhancement and irregular margins presage high-risk of NCR when the tumor size is greater than 5 cm. Above all, preoperative MR features and laboratory indicators can be applied to predict the early response of HCC to TACE/HIFU treatment and be considered in guiding therapeutic strategies to improve the prognosis of patients.

ACKNOWLEDGMENT

This work was supported by the National Natural Science Foundation of China (81401382) and the Medical Research Plan Project of Chongqing City House and Family Planning Committee in China (2016MSXM024). We deeply appreciate our colleagues at the HIFU Treatment Center and Clinical Laboratory for their close cooperation in data collection and technical consultations and American Journal Experts (AJE) for assistance with language editing.

REFERENCES

1. Stampfl U, Bermejo JL, Sommer CM, Hoffmann K, Weiss KH, Schirmacher P, et al. Efficacy and nontarget effects of transarterial chemoembolization in bridging of hepatocellular carcinoma patients to liver transplantation: a histopathologic study. *J Vasc Interv Radiol* 2014; **25**: 1018–26. doi: https://doi.org/10.1016/j.jvir.2014.03.007
2. Herber S, Biesterfeld S, Franz U, Schneider J, Thies J, Schuchmann M, et al. Correlation of multislice CT and histomorphology in HCC following TACE: predictors of outcome. *Cardiovasc Intervent Radiol* 2008; **31**: 768–77. doi: https://doi.org/10.1007/s00270-007-9270-8
3. Cheung TT, Fan ST, Chu FSK, Jenkins CR, Chok KSH, Tsang SHY, et al. Survival analysis of high-intensity focused ultrasound ablation in patients with small hepatocellular carcinoma. *HPB* 2013; **15**: 567–73. doi: https://doi.org/10.1111/hpb.12025
4. Li C, Zhang W, Zhang R, Zhang L, Wu P, Zhang F. Therapeutic effects and prognostic factors in high-intensity focused ultrasound combined with chemoembolisation for larger hepatocellular carcinoma. *Eur J Cancer* 2010; **46**: 2513–21. doi: https://doi.org/10.1016/j.ejca.2010.06.015
5. Zhou Y, He L, Huang Y, Chen S, Wu P, Ye W, et al. CT-based radiomics signature: a potential biomarker for preoperative prediction of early recurrence in hepatocellular carcinoma. *Abdom Radiol* 2017; **42**: 1695–704. doi: https://doi.org/10.1007/s00261-017-1072-0
6. Lee S, Kim KA, Park M-S, Choi SY. MRI findings and prediction of time to progression of patients with hepatocellular carcinoma treated with drug-eluting bead transcatheter arterial chemoembolization. *J Korean Med Sci* 2015; **30**: 965–73. doi: https://doi.org/10.3346/jkms.2015.30.7.965
7. Ma XH, Wang S, Zhao XM, Ouyang H, Wang M, Zhu YJ, et al. The quantitative analysis of Mr dynamic contrast-enhangced imaging on efficacy and prognosis of transcatheter arterial chemoembolization on hepatocellular carcinoma. *Zhonghua Zhong Liu Za Zhi* 2017; **39**: 689–94. doi: https://doi.org/10.3760/cma.j.issn.0253-3766.2017.09.010
8. Park YS, Lee CH, Kim JH, Kim IS, Kiefer B, Seo TS, et al. Using intravoxel incoherent motion (IVIM) MR imaging to predict lipiodol uptake in patients with hepatocellular carcinoma following transcatheter arterial chemoembolization: a preliminary result. *Magn Reson Imaging* 2014; **32**: 638–46. doi: https://doi.org/10.1016/j.mri.2014.03.003
9. Lin M, Tian M-M, Zhang W-P, Xu L, Jin P. Predictive values of diffusion-weighted imaging and perfusion-weighted imaging in evaluating the efficacy of transcatheter arterial chemoembolization for hepatocellular carcinoma. *Onco Targets Ther* 2016; **9**: 7029–37. doi: https://doi.org/10.2147/OTT.S112555
10. Li Z, Xue T-Q, Chen X-Y. Predictive values of serum VEGF and CRP levels combined with contrast enhanced MRI in hepatocellular carcinoma patients after TACE. *Am J Cancer Res* 2016; **6**: 2375–85.
11. Ma W-jun, Wang H-yong, Teng L-song, , Wang HY, Teng LS. Correlation analysis of preoperative serum alpha-fetoprotein (AFP) level and prognosis of hepatocellular carcinoma (HCC) after hepatectomy. *World J Surg Oncol* 2013; **11**: 212. doi: https://doi.org/10.1186/1477-7819-11-212
12. Douhara A, Namisaki T, Moriya K, Kitade M, Kaji K, Kawaratani H, et al. Predisposing factors for hepatocellular carcinoma recurrence following initial remission after transcatheter arterial chemoembolization. *Oncol Lett* 2017; **14**: 3028–34. doi: https://doi.org/10.3892/ol.2017.6489
13. European association for the study of the liver, European Organisation for research and treatment of cancer. EASL-EORTC

clinical practice guidelines: management of hepatocellular carcinoma. *J Hepatol* 2012; **56**: 908–43.
14. Kudo M, Ueshima K, Kubo S, Sakamoto M, Tanaka M, Ikai I, et al. Response evaluation criteria in cancer of the liver (RECICL) (2015 revised version. *Hepatol Res* 2016; **46**: 3–9. doi: https://doi.org/10.1111/hepr.12542
15. Sullivan LM, Massaro JM, D'Agostino RB. Presentation of multivariate data for clinical use: the Framingham study risk score functions. *Stat Med* 2004; **23**: 1631–60. doi: https://doi.org/10.1002/sim.1742
16. Vesselle G, Quirier-Leleu C, Velasco S, Charier F, Silvain C, Boucebci S, et al. Predictive factors for complete response of chemoembolization with drug-eluting beads (DEB-TACE) for hepatocellular carcinoma. *Eur Radiol* 2016; **26**: 1640–8. doi: https://doi.org/10.1007/s00330-015-3982-y
17. Renzulli M, Brocchi S, Cucchetti A, Mazzotti F, Mosconi C, Sportoletti C, et al. Can current preoperative imaging be used to detect microvascular invasion of hepatocellular carcinoma? *Radiology* 2016; **279**: 432–42. doi: https://doi.org/10.1148/radiol.2015150998
18. Santambrogio R, Bruno S, Kluger MD, Costa M, Salceda J, Belli A, et al. Laparoscopic ablation therapies or hepatic resection in cirrhotic patients with small hepatocellular carcinoma. *Dig Liver Dis* 2016; **48**: 189–96. doi: https://doi.org/10.1016/j.dld.2015.11.010
19. Ohmoto K, Yoshioka N, Tomiyama Y, Shibata N, Kawase T, Yoshida K, et al. Comparison of therapeutic effects between radiofrequency ablation and percutaneous microwave coagulation therapy for small hepatocellular carcinomas. *J Gastroenterol Hepatol* 2009; **24**: 223–7. doi: https://doi.org/10.1111/j.1440-1746.2008.05596.x
20. Ariizumi S-ichi, Kitagawa K, Kotera Y, Takahashi Y, Katagiri S, Kuwatsuru R, et al. A non-smooth tumor margin in the hepatobiliary phase of gadoxetic acid disodium (Gd-EOB-DTPA)-enhanced magnetic resonance imaging predicts microscopic portal vein invasion, intrahepatic metastasis, and early recurrence after hepatectomy in patients with hepatocellular carcinoma. *J Hepatobiliary Pancreat Sci* 2011; **18**: 575–85. doi: https://doi.org/10.1007/s00534-010-0369-y
21. An C, Kim DW, Park Y-N, Chung YE, Rhee H, Kim M-J. Single hepatocellular carcinoma: preoperative MR imaging to predict early recurrence after curative resection. *Radiology* 2015; **276**: 433–43. doi: https://doi.org/10.1148/radiol.15142394
22. Kim H, Park M-S, Choi JY, Park YN, Kim M-J, Kim KS, et al. Can microvessel invasion of hepatocellular carcinoma be predicted by pre-operative MRI? *Eur Radiol* 2009; **19**: 1744–51. doi: https://doi.org/10.1007/s00330-009-1331-8
23. Li T, Wang S-K, Zhou J, Sun H-C, Qiu S-J, Ye Q-H, et al. Positive HBcAb is associated with higher risk of early recurrence and poorer survival after curative resection of HBV-related HCC. *Liver Int* 2016; **36**: 284–92. doi: https://doi.org/10.1111/liv.12898
24. Matsui O, Kobayashi S, Sanada J, Kouda W, Ryu Y, Kozaka K, et al. Hepatocelluar nodules in liver cirrhosis: hemodynamic evaluation (angiography-assisted CT) with special reference to multi-step hepatocarcinogenesis. *Abdom Imaging* 2011; **36**: 264–72. doi: https://doi.org/10.1007/s00261-011-9685-1
25. Choi J-Y, Lee J-M, Sirlin CB. CT and MR imaging diagnosis and staging of hepatocellular carcinoma: Part II. Extracellular agents, hepatobiliary agents, and ancillary imaging features. *Radiology* 2014; **273**: 30–50. doi: https://doi.org/10.1148/radiol.14132362
26. Li J, Zhu WL, Kang XX, Zheng L, Guo CY, Yu P, et al. Prognostic factors and model of primary liver cancer treated with transcatheter arterial chemoembolization combined with radiofrequency ablation. *Zhonghua Zhong Liu Za Zhi* 2017; **39**: 787–91. doi: https://doi.org/10.3760/cma.j.issn.0253-3766.2017.10.013
27. Murakami M, Nagano H, Kobayashi S, Wada H, Nakamura M, Marubashi S, et al. Effects of pre-operative transcatheter arterial chemoembolization for resectable hepatocellular carcinoma: implication of circulating cancer cells by detection of α-fetoprotein mRNA. *Exp Ther Med* 2010; **1**: 485–91. doi: https://doi.org/10.3892/etm_00000076
28. El-Serag HB, Marrero JA, Rudolph L, Reddy KR. Diagnosis and treatment of hepatocellular carcinoma. *Gastroenterology* 2008; **134**: 1752–63. doi: https://doi.org/10.1053/j.gastro.2008.02.090
29. Memon K, Kulik L, Lewandowski RJ, Wang E, Ryu RK, Riaz A, et al. Alpha-fetoprotein response correlates with EASL response and survival in solitary hepatocellular carcinoma treated with transarterial therapies: a subgroup analysis. *J Hepatol* 2012; **56**: 1112–20. doi: https://doi.org/10.1016/j.jhep.2011.11.020
30. Jeong Y, Yoon SM, Han S, Shim JH, Kim KM, Lim Y-S, et al. Propensity score matching analysis of changes in alpha-fetoprotein levels after combined radiotherapy and transarterial chemoembolization for hepatocellular carcinoma with portal vein tumor thrombus. *PLoS One* 2015; **10**: e0135298: e0135298: . doi: https://doi.org/10.1371/journal.pone.0135298
31. Shen J-Y, Li C, Wen T-F, Yan L-N, Li B, Wang W-T, et al. Alpha fetoprotein changes predict hepatocellular carcinoma survival beyond the Milan criteria after hepatectomy. *J Surg Res* 2017; **209**: 102–11. doi: https://doi.org/10.1016/j.jss.2016.10.005
32. Jolesz FA. MRI-guided focused ultrasound surgery. *Annu Rev Med* 2009; **60**: 417–30. doi: https://doi.org/10.1146/annurev.med.60.041707.170303